Small unmanned aerial model accuracy for photogrammetrical fluvial bathymetric survey

Entwistle Neil[a*], Heritage George[a]

University of Salford, School of Environment and Life Sciences, Peel Building, Salford, UK, M5 4WT

Fluvial systems offer a challenging and varied environment for topographic survey, displaying a rapidly varying morphology, vegetation assemblage and degree of submergence. Traditionally theodolite or GPS based systems have been used to capture cross-section and breakline based topographic data which has subsequently been interpolated. Advances in survey technology has resulted in an improved ability to capture larger volumes of information with infrared terrestrial and aerial LiDAR systems capturing high-density (<0.02 m) point data across terrestrial surfaces. The rise of Structure from Motion (SfM) photogrammetry, coupled with small unmanned aerial vehicles (sUAV), has potential to record elevation data at reach scale sub decimetre density. The approach has the additional advantage over LiDAR of seeing through clear water to capture bed detail, whilst also generating ortho-rectified photographic mosaics of the survey reach. However, data accuracy has yet to be comprehensively assessed. Here we present a survey protocol for sUAV deployment and provide a reach scale comparison between a theodolite and SfM sUAV survey on the River Sprint, Kendal, the River Ehen at Egremont, England and the Afon Elwy, at Llanfair Talhaiarn, Wales. Comparative analysis between theodolite survey and SfM suggest similar accuracy and precision across terrestrial surfaces with error lowest over solid surfaces, increasing with vegetation complexity. Submerged SfM data, captured bed levels generally to within ±0.25 m with only a weak relationship recorded between error and flow depth. Significantly, associated error when linked to channel D_{50} highlights the ability of unmanned aerial vehicles to capture accurate fluvial data across a range of river biotopes and depths to 2.4 m.

Keywords: UAV, SfM, Biotopes, surveying

*Entwistle Neil, Email *N.S.Entwistle@salford.ac.uk*

1. Introduction

New techniques for rapid and detailed spatial data collection combined with sophisticated spatial analytical software facilitates the construction of Digital Elevation Models (DEMs) that accurately represent landform surface variability and offer an increased ability to measure and monitor morphological change across a range of spatial scales (Brasington et al., 2000; Fuller et al., 2005). Fluvial systems offer a challenging and varied environment for topographic survey, displaying a rapidly varying morphology, diverse vegetation assemblage and varying degree of inundation. Traditionally theodolite or GPS based systems have been used to capture cross-section and break of slope-based data which are subsequently interpolated to generate a topographic surface. Advances in survey technology has resulted in an improved ability to capture larger volumes of data with infrared terrestrial and aerial LiDAR systems capturing high-density (<0.02 m) data across terrestrial surfaces (Heritage and Hetherington, 2007; Bangen et al., 2014; Entwistle et al. 2018) but instruments are expensive and cumbersome and generally fail to survey through water resulting in a lack of bathymetric data (Milan et al., 2010). The issue of measurement through water has to some degree been overcome through the advent of Structure from Motion (SfM) photogrammetry, coupled with small unmanned aerial vehicles (sUAV) and there is now the potential to rapidly record the information needed to derive elevation data at a reach scale with sub decimetre density, seeing through clear water to capture bed detail (Entwistle et al., 2018).

Software utilising the photogrammetry Structure-from-Motion workflow (SfM) photogrammetry workflow facilitates the utilization of this technique by non-specialists allowing high-resolution morphometric 3D models and derived products such as digital surface models (DSMs) and orthophotographs to be produced (see Westoby et al., 2012;

Fonstad et al., 2013; Micheletti et al., 2014; Carrivick et al., 2016; Entwistle and Heritage, 2017).

There has been a recent proliferation in publications assessing the accuracy of SfM-derived data studies (for example Entwistle and Heritage, 2017, Harwin and Lucieer, 2012; James and Robson, 2012; Westoby et al., 2012; Fonstad et al., 2013; Tonkin et al., 2014; Smith and Vericat, 2015; Brunier et al., 2016, James and Quinton, 2014; Stumpf et al., 2015). Reported accuracies vary widely, from <0.1 m to over 1 m, with error attributed variously to image resolution/quality, image distortion, camera calibration and to the characteristics of the surface being measured particularly with respect to vegetation (see Harwin and Lucieer, 2012; James and Robson, 2012; Westoby et al., 2012; Fonstad et al., 2013; James and Quinton, 2014; Tonkin et al., 2014; Smith and Vericat, 2015; Stumpf et al., 2015; Brunier et al., 2016; Entwistle and Heritage 2017).

Of interest is the lack of studies reviewing the accuracy of SfM photogrammetry bathymetric data. Woodget et al., (2015) surveyed the River Arrow and Coledale Beck in the UK to produce digital elevation models at 0.02 m resolution reporting error on submerged areas between 0.016 m to 0.089 m, reducing to 0.008 m to 0.053 m when corrected for refraction. Woodget et al., (2017a) report near continuous underestimation of water depth from sUAV based image photogrammetry for the River Teme and a study by Dietrich (2017) reduced error on bathymetric data to 0.01 m or less on the White River, Vermont using a spatially varied refraction correction. This study builds on their work through the collection and analysis of bathymetric data from three contrasting watercourses capturing a variety of hydraulic habitats. The accuracy of the data are assessed against theodolite measurements.

1.1 Approaches to bathymetric survey

Theodolite based survey techniques and Global Positioning by Satellite (GPS) instruments have traditionally been used for shallow water bathymetric mapping (Woodget et al., 2015). Such point-based survey techniques, whilst accurate, are time consuming (Winterbottom and Gilvear, 1997) and the sparse data sets require careful interpolation to achieve a realistic surface representation (Fuller et al., 2003). They have also been shown to suffer from operator bias (Heritage and Hetherington 2007).

Several remote sensing techniques are also able to collect data over submerged surfaces. Spectral depth approaches rely on an empirical relationship between the spectral absorption properties of water and water depth. Using this technique Lejot et al., (2007) achieved bathymetric measurements at a 0.05m resolution with elevation error generally below 0.1m through water depths up to 1 m. However, other researchers have noted that the technique requires field data collection for calibration and have documented issues associated with turbidity, water surface disruption, illumination angle and substrate type (Winterbottom and Gilvear 1997; Westaway et al., 2003; Legleiter et al., 2004; Carbonneau et al., 2006; Lejot et al., 2007; Legleiter et al., 2009; Bergeron and Carbonneau 2012; Legleiter, 2012).

Terrestrial Laser Scanning (TLS) has emerged as a valuable technique in the fields of fluvial geomorphology and hydromorphology, providing means to acquire high precision, three-dimensional topographic data at resolutions previously unobtainable by conventional monitoring techniques. In addition, recent advances in analytical apparatus, computer software and computational ability have permitted construction of complex digital elevation models (DEMs) that accurately represent variability of landform through time (Heritage and Hetherington, 2007). In turn, this provides an opportunity to measure and monitor, quantifiably, morphological change at various spatial and temporal scales (Marcus and Fondstad, 2010). Whilst these studies have elucidated the benefits of TLS, they have typically been of limited areal coverage (e.g. Resop and Hession, 2010). In addition, a number of limitations in its application including absorption and refraction over water (Wheaton, 2008) and vegetation (Heritage and Hetherington 2007) must be considered.

Airborne Lidar systems are emerging as major sources of topographic data and faster systems are achieving data density comparable to older terrestrial systems. The laser pulse is also capable of canopy penetration, overcoming a significant limitation in terms of photogrammetry for DEM generation. Kraus and Pfeifer (1998) demonstrated that the accuracy of LiDAR- derived DEM in forested areas is equivalent to that of photogrammetry-derived DEM across open areas. The common use of eye safe near infra-red laser sources result in absorption and refraction issues with water (Legleiter, 2012). Blue-green scanning approaches are less affected by turbidity and water surface roughness than passive remote sensing techniques (Marcus, 2012). This is partially due to active blue-green lasers being less affected by turbidity and water surface roughness (Marcus, 2012), however their pulse footprint is larger than for infra-red lasers and instruments are currently expensive. Estimation of gravel-bed river bathymetry from space has been accomplished using a variety of methods, as an example Legleiter et al., (2009) utilised hyperspectral image data and a spectrally based remote sensing algorithm to gain results that were spatially coherent, although greater error was found at channel margins where pixels mixed. Yoon et al., (2012) estimated bathymetry using data from the Surface Water and Ocean Topography (SWOT) satellite to improve simulation of discharge, but only on large rivers (> 50 m wide), however Biancamaria et al (2016) review other land hydrology capabilities of SWOT, including those related to transboundary river basins, human water withdrawals and wetland environments.

Others have used satellite data to map habitats (Hugue et al., 2016), for flood forecasting (García-Pintado et al., 2015) and to advance river modelling in ungauged basins (Maswood and Hossain, 2016).

Digital photogrammetry is now widely used to capture topographic data with data resolution and positional accuracy dependent on image resolution and distance of capture. Early work used terrestrial photogrammetry to produce dense accurate morphometric data, but areal coverage was restricted by the camera field of view (Heritage et al.,2009). The recent development of small unmanned aerial vehicles and associated software advances have improved coverage and many studies are now published on its use across a range of environments (see Harwin and Lucieer, 2012; James and Robson, 2012; Westoby et al., 2012; Fonstad et al., 2013; Tonkin et al., 2014; Smith and Vericat, 2015; Brunier et al., 2016, James and Quinton, 2014; Stumpf et al., 2015). Issues have been reported with light penetration and inaccurate positioning due to refraction through the water column. Westaway et al., (2001) partially overcame this using simple refraction correction and Dietrich (2017) further refined the correction process using spatially varying refraction rectification. Both approaches have helped adjust elevation predictions and improve depth estimation across submerged surfaces.

2. Study sites

Three sites were used in this study to assess the accuracy of photogrammetric estimation of water depth using imagery obtained from sUAV survey reflecting a diversity of fluvial environments. These were the River Sprint and River Ehen in Cumbria, England and the Afon Elwy in Wales, (Figure 1).

Figure 1. Location for the three sites used in this study to reflect a diversity of fluvial environments, A) River Sprint, Cumbria, England. B) Afon Elwy, North Wales, C) River Ehen, Cumbria, England.

2.1 River Sprint

The Sprint is a small river with a catchment area of around 35 km^2 joining the River Kent just south of Burnside in the English Lake District. Average rainfall in the catchment is very high, amounting to 2,018 mm per year. Flow has been recorded at Sprint Mill since 1976, located just upstream of the confluence with the River Kent. Median flow there is around 1.0 m^3s^{-1}, whilst the Q95 (typical summer flow) is around 0.17 m^3s^{-1} and the Q10 (typical winter flow) is around 4.8 m^3s^{-1}. The land use and habitat of the catchment is >80% grassland, approximately 10% mountainous, heath or bog with around 6% woodland, with a history of slate mining in the upper catchment and a number of steep coarse-bedded tributaries. These tributaries drain the surrounding fells delivering a coarse sediment load onto a flatter wider piedmont zone below where transport energy drops off rapidly creating a long (>750 m) depositional zone at the Sadghyll gravel trap study site (Figure 2a). This area is characterised by a wide coarse-sediment covered valley floor dissected by multiple active and inactive distributary channels (Figure 2b). The bathymetric survey captured data in pool areas. A combined sUAV and theodolite survey generated a DEM for the site (Figure 2c) the characteristics of which are given in Table 1. Local Wolman samples suggest a general medium gravel size distribution (D_{16} 0.024 m, D_{50} 0.055 m, D_{84} 0.103 m).

Figure 2. River Sprint sUAV derived orthophoto (A) and Digital Terrain Model (B) including boundary of pool area used for bathymetry data analysis.

2.2 Afon Elwy

The Elwy is the largest sub-catchment of the Clwyd catchment in North Wales. The confluence of the Afon Elwy with the Afon Clwyd is downstream of St Asaph. The study site is located at Bryn Yr Ur the on the main river. The watercourse here is characterised by a low sinuosity single thread channel with occasional bifurcations around gravel/cobble shoals. The study site was located at a bifurcation displaying a high morphologic and hydraulic diversity. Data were captured across, riffle, pool, glide, chute and backwater zones (Figure 3) considering a variety of surface water biotopes and a range of depths. A combined sUAV and theodolite survey generated a DEM for the site the characteristics of which are given in Table 1. Local Wolman samples suggest a general medium gravel size distribution (D_{16} 0.03 m, D_{50} 0.049 m, D_{84} 0.107 m).

Figure 3. Afon Elwy sUAV derived orthophoto (A) and Digital Terrain Model (B). Inset image delimits the area used for biotope-based bathymetry data analysis.

2.3 River Ehen

The study area at Egremont lies within the lower part of the River Ehen, approximately 10 km downstream from its source at the outflow of Ennerdale Lake. The river, in the vicinity of Egremont, Cumbria is an active single thread channel that has historically been heavily modified to stabilise the channel planform and to utilise the power of the water flow for industry. Median flow from records at Braystones (1974-2014) is around 70 m^3s^{-1}, whilst the Q95 (typical summer flow) is around 0.96 m^3s^{-1} and the Q10 (typical winter flow) is around 11.9 m^3s^{-1}. The study site is located across a transverse bar upstream of Ennerdale Mill Dam Weir (Figure 4) allowing data to be captured across an extensive riffle area and associated rapidly flowing chute and a shallow pool zone. A combined sUAV and theodolite survey generated a DEM for the site the characteristics of which are given in Table 1. Local Wolman samples suggest a general medium gravel size distribution (D_{16} 0.038 m, D_{50} 0.068 m, D_{84} 0.153 m).

Figure 4. River Ehen sUAV derived orthophoto (A) and Digital Terrain Model (B) showing the area used for bathymetry data analysis.

Table 1. Site survey characteristics for the three study sites

3. Method

3.1 sUAV Data acquisition

A small unmanned aerial vehicle (sUAV) (DJi quadcopter – Phantom 3 professional) was used to obtain multiple aerial photographs of each study reach using a high-resolution (12.76 Megapixels, at an image size resolution of 4000×3000). 94° of a 20mm field of view was utilised by the on board 1/2.3” CMOS digital camera sensor, which is mounted on a remotely operated 3 axis gyroscopic gimble to allow for optimal stability during flight reducing blur issues on the captured imagery (see Woodget et al., 2017b). Remote activation ensured sufficient spatial coverage and substantial image overlap (following the SfM principles of Micheletti et al., 2014). Further, manual flying minimised the likelihood of unfocussed images though maintaining a consistent flight height, controlling speed, curtailing external influences and ensuring sUAV stability for focused photographs.

The importance of camera settings for standard photogrammetry has been reviewed by James et al. (2017) and survey settings were optimized for light conditions for each study reach, these included: ISO levels, exposure compensation, white balance, and capture format.

The sUAV was operated by a UK Civil Aviation Authority approved qualified drone capturing (>80%) overlapping nadir images. This was supplemented with a range of off-nadir images across the study reaches. The sUAV was flown at uniform height (~30 m, 100 ft) to allow for accurate reconstruction during post-processing, although external influences, such as significant air turbulence, can affect the vertical hover accuracy, flights for this research were flown in optimal conditions and a hover accuracy range resulted in a ±0.1 m margin. Operator experience suggests that this altitude was optimal for day survey of a river and floodplain with a combined width of around 250 m.

High quality survey georeferencing was achieved through a system of ground control points (GCPs) spaced roughly equidistant around 10 channel widths apart through the survey area. Such a systematic distribution maximises their effectiveness in post-processing (Tonkin and Midgley, 2016), whilst James and Robson (2014) highlighted the importance of well-focussed, similar distance, imagery of consistent surface texture and as the important factor in accurate DEM construction, facilitating survey accuracy and reducing the overall number of GCPs required. GCPs and real-world bathymetric ground points in this research were surveyed using a calibrated TopCon GTS-210 EDM theodolite (±0.01 m accuracy) to provide a robust local coordinate system for each model and to test the bathymetric accuracy

3.2 Post-processing of sUAV data

All post-processing was conducted on Intel Xeon desktop computer with 256Gb RAM using Agisoft Structure from Motion (SfM) professional software. Images were mosaicked together using a SfM photogrammetry approach (Micheletti et al., 2015) whereby rasterized three-dimensional representations are constructed from two-dimensional (camera calibrated) images (see Scaramuzza et al., 2006).

Images were manually inspected for quality, with out-of-focus or blurred photographs discarded. Whilst Agisoft's image quality algorithm can automatically analyse images using the contrast between pixels to determine image quality, camera blur is often directional and as a result some sharp edges can remain. Therefore using the Image Quality function estimated quality is not necessarily a meaningful value for sharpness. All images were subsequently cropped to utilise only the central (90%) area, this reduced any lens image distortion effects (Wackrow and Chandler, 2011) on the final model. Images were then aligned through the automated SfM software through identification of conjugate points common in several photographs. This was propagated over the all of the study reaches. SfM photogrammetry strategies suggest that fewer systematic errors are a direct result of combining nadir and off-nadir image datasets (James and Robson, 2014; Dietrich 2017).

Within each aerial image, the ground control points were manually assigned their corresponding theodolite-derived coordinate in the SfM software allowing the photographs to be realigned and scaled based on the local theodolite coordinate system. Dense point clouds were then built from the geo-rectified imagery using depth filtering to remove the lowest number of points which do not belong to a connected surface. This ignores unnecessary micro-scale details during processing, thereby decreasing computing time. Geometry was constructed using a height field approach and disabled interpolation yielded geometry based on points constructed in the dense point cloud. A textured model was then built using the previously computed geometry. Here, raw image pixels were draped over the geometric model to yield a DEM. In addition, this process provided fully orthorectified aerial images of each study reach.

To support accurate data comparison the sUAV survey approach followed the protocol set by Heritage and Hetherington (2007) and successfully adopted in a pool-riffle study by Entwistle (2011) whereby the channel and surrounding floodplain were surveyed to a single project coordinate system using the independent theodolite points and set to a point spacing of 0.02 m. The resultant meshed set of UAV derived data points were clipped to remove unwanted information such as distant points, overhanging tree canopy and any spurious aerial data points.

3.3 Water Surface and Depth data collection

A theodolite survey was conducted at each site to capture independent depth measurements across a range of submerged topography in the same coordinate system as the sUAV survey, Table 2 summarises the data collected. The reflector pole was placed on the bed of the channel, and then raised to the level of the water surface in the same place allowing flow depth to be computed from the difference between the two values. In addition, water edge points were surveyed to compute a water elevation surface map and sUAV points corresponding to the theodolite depth values were subtracted from this surface to generate a depth estimate from the sUAV approach.
Comparative data points were collected across each study site to reflect hydraulic biotopes present (sensu Newson and Newson, 2000) allowing the sUAV data to be evaluated across each of these flow types. These data are summarised in table 2, numbers of points reflect the size and distribution of each biotope type at each site.

Table 2. Measured water depth data characteristics for the three study sites

3.4 Bed Roughness Estimation

Each sUAV surface point cloud was interrogated through filtering a moving window standard deviation (equivalent to the calibre of the largest grains observed in the field) to generate a surface roughness map of the surveyed sites. These data were multiplied by 2 to generate an approximation of the grain protrusion characteristics (see Gomez 1995; Entwistle and Fuller, 2009; Heritage and Milan 2009). These data were then investigated to extract the roughness values (C axis) at each of the depth measurement points for later comparison against the depth estimation error.

4. Results

4.1 Model build characteristics

Summary statistics of the general survey for each study site are presented in Table 1. It is clear that the SfM technique is able to locate georeferenced GCP sites to a high level of accuracy (RMSE <± 0.019 m) comparable with that reported by James and Robson, (2014); Fonstad et al., (2013); Dietrich (2017). The data point density may be controlled within the SfM software up to the pixel resolution on the captured images with higher density point clouds requiring considerably increased post-processing time and computing power. To overcome computational limitations, or reduce processing time on standard desktop machines, the point cloud can be extracted from the SfM software and imported into CloudCompare (Girardeau-Montaut, 2018) freeware to build a structured point cloud and generate the mesh for DEM construction.

4.2 Overall sUAV Error associated with Submerged Surfaces

sUAV derived depth estimates and those measured with the theodolite were comparatively plotted (Figure 5). Depths up to 2.4 m were measured with the majority falling below 1.75 m. Whilst some scatter appears in the data. The distribution of difference (Figure 6) statistics reveal a low mean error of 0.04 m, the data are skewed slightly to the right of this mean with a tail of more positive error (skew = 0.224). The tails on the error are relatively large with the data displaying a kurtosis value of -0.229.

Figure 5. Comparative theodolite and sUAV depth data for the three study rivers. The solid line represents equality and dashed lines ±10% difference.

Figure 6. Theodolite and sUAV estimate depth discrepancy for Rivers Sprint A) Ehen B) and Elwy C).

The difference between the sUAV and theodolite values are calculated independently for each study site (Figure 7a-c). For the River Sprint (Figure 7a) the relationship is strongly linear (r^2 0.85) with a 1.02 multiplier on the regression line up to depths of 1m suggesting that the sUAV depths closely match the theodolite values across all depths. Error bands have been included on the graph representing the D_{84} grainsize measured at the site and the majority of error occurring within these bounds. The errors recorded on the Afon Elwy are shown in Figure 7b; again, the relationship is a strong linear one (r^2 0.88), however, here there is a consistent underestimation of depth relative to the theodolite data. This may in part be due to refraction, however, there does not appear to be a trend of increasing difference with measured depth (up to 0.8 m depths measured) with the trend on the data and a refraction correction of 1.2 on the sUAV data would provide optimal depth prediction. Error bands have been included on the graph representing $\pm D_{84}$ grainsize measured at the site. This characteristic continues with the error plot for the River Ehen (Figure 7c) up to depths of around 1.5 m. After this error is seen to increase above that which could be attributed to the general bed roughness. A linear regression relationship also best described these data (r^2 0.89) with a multiplier of 0.8 suggesting minor under prediction of depth by the sUAV

Figure 7. sUAV model estimate depth discrepancy relationship with measured depth for the a) River Sprint, b) Afon Elwy and c) River Ehen. Solid line represents regression, dashed lines equivalent to D_{84} grain size error.

4.3 sUAV Error and Local Bed Roughness

Figure 8 illustrates the bed roughness variability across the three study sites as defined by the local standard deviation of the sUAV point cloud. These data were multiplied by 2 to generate an approximation of the grain protrusion characteristics (see Gomez 1995, Heritage and Milan, 2009; Entwistle and Fuller, 2009). The majority of the area subject to theodolite survey exhibits surface roughness variation up to 0.2 m. The River sprint is generally finest with the Afon Elwy exhibiting a finer apical pool area and smaller gravels are associated with a developing transverse bar feature towards the upstream survey extent on the River Ehen. These roughness values are less than those measured using a Wolman count as they are more characteristic of the sediment c-axis

Figure 8. Bed roughness characteristics calculated by a moving window standard deviation across the DM surface for a) River Sprint, b) Afon Elwy and c) River Ehen.

The local grain surface roughness character was extracted for each theodolite measurement point for all three rivers and these data were plotted against the error on the sUAV data compared to the theodolite survey (Figure 9). On the River Sprint the majority of the roughness data are below 0.3 m. The Afon Elwy plot shows a near random distribution of error compared to bed roughness (liner regression r^2 0.1). The River Ehen suggests greatest error (up to 0.3 m) across areas of finer sediment (< 0.05 m) before showing no relationship across rougher surfaces (Figure 9c).

Figure 9. Local bed roughness associated with measured sUAV error across a) River Sprint, b) Afon Elwy and c) River Ehen.

This general absence of any relationship between sUAV error and grainsize suggest that it is unlikely that theodolite error is playing any major role in influencing the evaluation of the accuracy of the sUAV survey. It also suggested that the sUAV survey accuracy is also unaffected by bed roughness with the resolution on the survey sufficient to record local bed surface variation.

4.4 sUAV Error and Local Hydraulic Roughness

Error in the sUAV data was further investigated with respect to water surface conditions. Whilst water surface variation was not directly measured it can be inferred from the biotope distribution recorded at each site. As mentioned previously biotope types were assigned to each theodolite survey point during site survey and these were confirmed through interrogation of the sUAV orthophoto. For example, Milan et al. (2010) used water surface roughness delimiters to map hydraulic biotopes and through sUAV orthophoto analysis water surface roughess was seen to increase through pool, backwater, glide, run, riffle, chute biotope units.

The spatial variation in sUAV error is shown for all three study sites in Figure 10. This error is overlain on the biotope distribution. For the River Sprint there is a strong tendency for the sUAV depth estimates to exhibit high error across chute units (Figure 10a). On the Afon Elwy (Figure 10b) error is generally lower with pools exhibiting the worst depth predictions, this may reflect the general lower energy biotope ensemble present during the survey. sUAV error on the River Ehen was highest across the weir zone where chuting flow dominated and was also recorded along channel margins characterised by a well-developed woody riparian (Figure 10c).

Figure 10. Water surface roughness and sUAV depth error on a) River Sprint, b) Afon Elwy and c) River Ehen.

The apparent links between sUAV depth estimation error and hydraulic conditions was investigated further through categorisation of the depth data by observed hydraulic biotope. Plotting the sUAV error against measured depth for each biotope (Figure 11) and linear regression lines were fitted to each hydraulic habitat. The slope each line reflects the degree of difference between the two measures and these are summarised in Table 3.

Figure 11. sUAV and theodolite depth measurements split by hydraulic biotope for a) River Sprint, b) Afon Elwy and c) River Ehen.

Table 3. Linear regression multipliers on sUAV depth error estimates for the study sites on the River Sprint, Afon Elwy and River Ehen.

Shallow backwaters displaying no discernible water surface disruption appear to show near agreement between the theodolite and sUAV depth measurements. This is also true of the riffle areas, despite considerable water surface disruption and this is attributed to the shallow nature of these features effectively minimising refraction issues. This is not true of chute features where white water is severely impacting on bed visibility and the disrupted water surface is adding further complexity to refraction angles resulting in generally poor depth prediction from the sUAV survey. Glide and run linear regression multipliers range between 0.7 and 0.9 suggesting a general slight under prediction of depth.

5. Discussion

In this paper we have investigated the accuracy of structure from motion digital elevation model using imagery collected from an sUAV platform. The three rivers studied exhibited measured depths up to 2.4 m extending the evaluation beyond the depths of 1.1 m, 0.7 m and ~1.5 m reported by Westaway et al., (2001), Woodget et al., (2015) and Dietrich (2017) respectively and cover a wide range of hydraulic roughness elements ranging from pools through to chuting flow.

Individual histograms of mean average error on depth prediction by the sUAV at each of the survey sites are shown in Figure 6, a combined dataset generated a mean average error on depth prediction by the sUAV of ±0.03m (σ ±0.12 m), with individual data of River Sprint ±0.04 cm (σ 0.05), River Ehen ±0.03 (σ 0.12) and River Elwy ±0.03 cm (σ 0.06 cm) comparing favourably with the work of Westaway et al., (2001), who used conventional stereo photogrammetry to predict water depth achieving mean errors from 0.054 to 0.105 m with standard deviations of 0.092 to 0.116 m. This study did not apply a refraction correction to the data, preferring to investigate the degree to which refraction was influencing the predictive capability of the sUAV technique, however our uncorrected general results were comparable to those of Woodget et al., (2015), who used a simple refraction correction to achieve mean depth errors of 0.029 to 0.053 m (σ 0.064 to 0.086 m) and Dietrich (2017) applied a spatially varied refraction correction on two surveys of the White River achieving mean errors of -0.011 and 0. 014m with standard deviations of 0.077 and 0.059 m.

It is recognised that refraction through water can impact depth estimation and many authors have utilised the simple depth correction factor of 1.4 proposed by Westaway et al., 2001 and Woodget et al., (2015) argue for a refraction correction to improve sUAV depth estimation accuracy. Results from these studies showed an improvement in mean error following refraction correction, and for depths less than 0.4m mean error became comparable with that of exposed terrain. However, larger errors were observed at depths beyond 0.4m which scaled with depth (Westaway et al., 2000). This study has found that the level of error in the raw data is generally insufficient to warrant the application of any correction with errors in depth estimation within the range of bed roughness for all three study sites and measurement error on the water surface caused by turbulence. Shallow water error was recorded, however, the multiplier required to correct the depth estimates was closer to 1.2. Other regions characterised by a generally smooth water surface and depths up to a metre showed even stronger with only a 10% correction needed to increase the depth to that recorded by the theodolite survey. Higher energy flow areas create a more complex refraction effect, and this is discussed further below.

Water surface disruption is also a source of survey error using remotely sensed data (Milan et al. 2010). This is true for both the sUAV (et al., 2017b) and the theodolite approach (Heritage et al., 2009) where a disrupted surface or fast flowing water requires the surveyor to estimate the average height of a rapidly varying water level. This effect has not been directly quantified in this study, however the biotope categorisation of the data can be used as a surrogate measure for water surface roughness with roughness seen to increase in the sequence, pool, glide, run, riffle, chute. Examination of the statistical significance of the empirical depth relationships discussed earlier suggest much poorer relationships with the higher energy biotopes, most notably chutes where white water is common. Here the variability in depth prediction was highest, with regression correlation coefficients to between 0.6 and 0.7. This strongly suggests that optical approaches to characterising submerged surfaces should not be attempted over areas with rapidly varying water surface conditions.

A source of possible error in the depth estimation process exists in the choice of DEM resolution. Point spacing of 0.08 m was selected in the SfM software to avoid excessive processing times. These data must then be interpolated to generate the topographic and bathymetric surfaces and measured depth points falling across interpolated areas may be in error. This error is likely to be a function of the local surface roughness. Comparison of the sUAV error compared to measured bed sediment size suggests that the error is within that of the bed roughness as defined by the grain size D_{84}. When local bed roughness (defined by the standard deviation of the local elevation data on the DEM) was compared to the sUAV depth error, no relationship was found suggesting factors other than sediment size variability were influencing survey accuracy.

Finally of note were errors recorded along the banks of the River Ehen study site, where riparian trees formed a dense canopy obscuring direct imaging of the bed of the channel. Insufficient oblique imagery meant that this was not correctable. Where vegetation infringes on survey areas further concentration of camera images, from multiple angles should be fed into the SfM facilitating DEM construction.

6. CONCLUSION

The use of high resolution remote sensing from a UAV is an encouraging technique for quantifying the topography of fluvial environments at the meso-habitat scale. This study has critically evaluated the ability of sUAV survey data and subsequent DEM development using SfM point cloud generation to predict water depth and by inference to accurately map bathymetric surfaces in clear water. It has extended the published depth research to 2.4 m and has refined the data analysis to differentiate error according to hydraulic conditions. Linear regression relationships were found to best fit the error data suggesting that error estimates did not increase with depth. Error on the direct estimates showed a general under prediction, however, depth over predictions also occurred. These errors were generally within the bounds of the bed roughness as defined by the grain size D_{84}. When investigated at the biotope scale across all three study sites the regression relationships suggest potential depth error corrections of 1.1 to 1.2, these values are lower than that suggested by Westaway (2001) and suggest that applying such a correction to all data would result in less accurate depth estimation, most notably for pools/backwaters, glides, runs and riffles. Error on chute estimations were higher and certainly more varied and it would appear that water surface disruption is the key cause of this.

It would appear from the results that good depth estimation levels can be achieved using the sUAV approach described. Caution must be exercised, however, where hydraulic energy levels and/or water depths relative to bed roughness are high as this appears to significantly increase the impact of refraction. More generally DEM generation can also be significantly impacted by vegetation and care must be taken to ensure that sUAV imagery captures detail across all wet areas to ensure correct model build.

7. References

Bangen SG, Wheaton JM, Bouwes N, Bouwes B, Jordan C. 2014. A methodological intercomparison of topographic survey techniques for characterizing wadeable streams and rivers. *Geomorphology* 206: 343-361.

Bergeron, N. and Carbonneau, P.E. 2012. Geosalar: Innovative remote sensing methods for spatially continuous mapping of fluvial habitat at riverscape scale' In *Fluvial Remote Sensing for Science and Management*, Carbonneau, P.E. and Piegay, H. (eds). Wiley-Blackwell, Chichester

Biancamaria, S., Lettenmaier, D.P. and Pavelsky, T.M., 2016. The SWOT mission and its capabilities for land hydrology. In *Remote Sensing and Water Resources* (pp. 117-147). Springer, Cham.

Brasington, J., Rumsby, B.T. and McVey, R.A., 2000. Monitoring and modelling morphological change in a braided gravel-bed river using high resolution GPS-based survey. *Earth Surface Processes and Landforms*, *25*(9), 973-990.

Brunier, G., Fleury, J., Anthony, E.J., Gardel, A. and Dussouillez, P., 2016. Close-range airborne Structure-from-Motion Photogrammetry for high-resolution beach morphometric surveys: Examples from an embayed rotating beach. *Geomorphology*, *261*, 76-88.

Carbonneau, P.E., Lane, S.N. and Bergeron, N., 2006. Feature based image processing methods applied to bathymetric measurements from airborne remote sensing in fluvial environments. *Earth Surface Processes and Landforms*, *31*(11), 1413-1423.

Carrivick, J.L., Smith, M.W. and Quincey, D.J., 2016. *Structure from Motion in the Geosciences*. John Wiley & Sons.

Dietrich, J.T., 2017. Bathymetric Structure-from-Motion: extracting shallow stream bathymetry from multi-view stereo photogrammetry. *Earth Surface Processes and Landforms*, *42*(2), 355-364.

Entwistle, N. S. (2011). *Geomorphological effectiveness and maintenance of a riffle-pool sequence* (Doctoral dissertation, Salford: University of Salford).

Entwistle, N.S. and Fuller, I.C., 2009. Terrestrial laser scanning to derive the surface grain size facies character of gravel bars. *Laser Scanning for the Environmental Sciences,* Chichester: Wiley, 102-114.

Entwistle, N.S. and Heritage, G., 2017. An evaluation DEM accuracy acquired using a small unmanned aerial vehicle across a riverine environment. *International Journal of New Technology and Research*, *3*(7): 43-48.

Fonstad MA, Dietrich JT, Courville BC, Jensen JL, Carbonneau PE. 2013. Topographic structure from motion: a new development in photogrammetric measurement. *Earth Surface Processes and Land-forms* 38(4): 421–430.

Fuller, I.C., Large, A.R.G., Charlton, M.E., Heritage, G.L. & Milan, D.J. (2003) Reach-scale sediment transfers: an evaluation of two morphological Budgeting approaches. *Earth Surface Processes & Landforms*. **28**, 889-904.

Fuller, I.C., Large, A.R.G., Heritage, G.L., Milan, D.J. and Charlton, M.E. 2005. Derivation of annual reach-scale sediment transfers in the River Coquet, Northumberland, UK, *International Association of Fluvial Sedimentologists Special Publication*, 35, 61-74.

García-Pintado, J., Mason, D. C., Dance, S. L., Cloke, H. L., Neal, J. C., Freer, J., & Bates, P. D. 2015. Satellite-supported flood forecasting in river networks: A real case study. *Journal of Hydrology*, *523*, 706-724.

Girardeau-Montaut D. 2018. CloudCompare [online] Available from: http://www.cloudcompare.org/

Gomez, B., Mertes, L.A., Phillips, J.D., Magilligan, F.J. and James, L.A., 1995. Sediment characteristics of an extreme flood: 1993 upper Mississippi River valley. *Geology*, *23*(11), 963-966.

Harwin S, Lucieer A. 2012. Assessing the accuracy of georeferenced point clouds produced via multi-view stereopsis from unmanned aerial vehicle (UAV) imagery. *Remote Sensing* 4: 1573–1599.

Heritage G, Hetherington D. 2007. Towards a protocol for laser scanning in fluvial geomorphology. *Earth Surface Processes and Landforms* 32:66–74.

Heritage, G.L. and Milan, D.J., 2009. Terrestrial laser scanning of grain roughness in a gravel-bed river. *Geomorphology*, 113(1), 4-11.

Heritage, G.L., Milan, D.J., Large, A.R. and Fuller, I.C., 2009. Influence of survey strategy and interpolation model on DEM quality. *Geomorphology*, 112(3-4), 334-344.

Hugue, F., Lapointe, M., Eaton, B. C., & Lepoutre, A. 2016. Satellite-based remote sensing of running water habitats at large riverscape scales: Tools to analyze habitat heterogeneity for river ecosystem management. G*eomorphology*, *253*, 353-369.

James, M. R., & Robson, S. 2014. Mitigating systematic error in topographic models derived from UAV and ground-based image networks. *Earth Surface Processes and Landforms*, *39*(10), 1413-1420.

James, M. R., Robson, S., d'Oleire-Oltmanns, S., & Niethammer, U. 2017. Optimising UAV topographic surveys processed with structure-from-motion: Ground control quality, quantity and bundle adjustment, *Geomorphology* 280, 51-66.

James, M.R. and Quinton, J.N., 2014. Ultra-rapid topographic surveying for complex environments: the hand-held mobile laser scanner (HMLS). *Earth surface processes and landforms*, *39*(1), 138-142.

Kraus, K. and Pfeifer, N. 1998: Determination of terrain models in wooded areas with airborne laser scanner data. *ISPRS Journal of Photogrammetry and Remote Sensing* 53(4), 193-203.

Legleiter, C.J., 2012. Remote measurement of river morphology via fusion of LiDAR topography and spectrally based bathymetry. *Earth Surface Processes and Landforms*, *37*(5), 499-518.

Legleiter, C.J. and Overstreet, B.T., 2014. Measuring the Morphology and Dynamics of the Snake River by Remote Sensing. *University of Wyoming National Park Service Research Center Annual Report*, *37*(1), 12-20.

Legleiter CJ, Roberts DA, Marcus WA, Fonstad MA. 2004. Passive optical remote sensing of river channel morphology and in-stream habitat: physical basis and feasibility. *Remote Sensing of Environment* 93: 493–510.

Legleiter CJ, Roberts DA. 2009. A forward image model for passive optical remote sensing of river bathymetry. *Remote Sensing of Environment* 113: 1025–1045.

Lejot J, Delacourt C, Piegay H, Fournier T, Tremelo M-L, Allemand P. 2007. Very high spatial resolution imagery for channel bathymetry and topography from an unmanned mapping controlled platform. *Earth Surface Processes and Landforms* 32: 1705–1725.

Marcus, W.A., 2012. Remote Sensing of the Hydraulic Environment in Gravel-Bed Rivers. *Gravel-Bed Rivers: Processes, Tools, Environments*, 259-285.

Marcus WA, Fonstad MA. 2010. Remote sensing of rivers: the emergence of a subdiscipline in the river sciences. *Earth Surface Processes and Landforms* 35: 1867–1872

Maswood, M., & Hossain, F. 2016. Advancing river modelling in ungauged basins using satellite remote sensing: the case of the Ganges–Brahmaputra–Meghna basin. *International Journal of River Basin Management*, *14*(1), 103-117.

Micheletti N, Chandler JH, Lane SN. 2014. Investigating the geomorphological potential of freely available and accessible structure from-motion photogrammetry using a smartphone. *Earth Surface Processes and Landforms*, DOI: 10.1002/esp.3648

Milan DJ, Heritage GL, Large ARG, Entwistle NS. 2010. Mapping hydraulic biotopes using terrestrial laser scan data of water surface properties. *Earth Surface Processes and Landforms* 35: 918-931.

Milan, D.J., Heritage, G.L., Large, A.R. and Fuller, I.C., 2011. Filtering spatial error from DEMs: Implications for morphological change estimation. *Geomorphology*, *125*(1), 160-171.

Newson, M.D.& Newson, C.L., 2000 "Geomorphology, ecology and river channel habitat: mesoscale approaches to basinscale challenges". *Progress in Physical Geography*. 24, 195–217.

Pe'Eri, S., & Philpot, W. 2007. Increasing the existence of very shallow-water LIDAR measurements using the red-channel waveforms. *IEEE Transactions on Geoscience and Remote Sensing*, 45(5), 1217-1223.

Resop, J.P. and Hession, W.C., 2010. Terrestrial laser scanning for monitoring streambank retreat: Comparison with traditional surveying techniques. *Journal of Hydraulic Engineering*, *136*(10), 794-798.

Scaramuzza, D., Martinelli, A., & Siegwart, R. 2006. A flexible technique for accurate omnidirectional camera calibration and structure from motion. In *Fourth IEEE International Conference on Computer Vision Systems* (ICVS'06) (45-45). IEEE.

Smith, M.W. and Vericat, D., 2015. From experimental plots to experimental landscapes: topography, erosion and deposition in sub-humid badlands from structure-from-motion photogrammetry. *Earth Surface Processes and Landforms*, *40*(12), 1656-1671.

Stumpf, A., Malet, J.P., Allemand, P., Pierrot-Deseilligny, M. and Skupinski, G., 2015. Ground-based multi-view photogrammetry for the monitoring of landslide deformation and erosion. *Geomorphology*, *231*, 130-145.

Tonkin, T.N., Midgley, N.G., Graham, D.J. and Labadz, J.C., 2014. The potential of small unmanned aircraft systems and structure-from-motion for topographic surveys: A test of emerging integrated approaches at Cwm Idwal, North Wales. *Geomorphology*, *226*, 35-43.

Tonkin, T. N., & Midgley, N. G. 2016. Ground-Control Networks for Image Based Surface Reconstruction: An Investigation of Optimum Survey Designs Using UAV Derived Imagery and Structure-from-Motion Photogrammetry. *Remote Sensing*, 8(9), 786.

Wackrow, R. and Chandler, J.H. 2011. Minimising systematic error surfaces in digital elevation models using oblique convergent imagery. *Photogrammetric Record* 26 (133): 16-31

Westaway, R.M., Lane, S.N. and Hicks, D.M. 2001. Remote sensing of clear water, shallow, gravel-bed rivers using digital photogrammetry. *Photogrammetric Engineering and Remote Sensing* 67 (11): 1271-1281

Westoby, M.J., Brasington, J., Glasser, N.F., Hambrey, M.J. and Reynolds, J.M., 2012.

'Structure-from-Motion'photogrammetry: A low-cost, effective tool for geoscience applications. *Geomorphology*, *179*, 300-314.

Wheaton, J. M. 2008. *Uncertainty in morphological sediment budgeting of rivers*. An unpublished Doctor of Philosophy Thesis. University of Southampton, Southampton. 412p.

Wheaton, J.M., Brasington, J., Darby, S.E. and Sear, D.A., 2010. Accounting for uncertainty in DEMs from repeat topographic surveys: improved sediment budgets. *Earth Surface Processes and Landforms*, *35*(2), 136-156.

Winterbottom SJ, Gilvear DJ. 1997. Quantification of channel bed morphology in gravel-bed rivers using airborne multispectral imagery and aerial photography. *Regulated Rivers: Research & Management* 13: 489–499.

Woodget AS, Carbonneau PE, Visser F, Maddock IP. 2015. Quantifying submerged fluvial topography using hyperspatial resolution UAS imagery and structure from motion photogrammetry. *Earth Surface Processes and Landforms* 40: 47–64.

Woodget, A.S. and Austrums, R., 2017a. Subaerial gravel size measurement using topographic data derived from a UAV-SfM approach. *Earth Surface Processes and Landforms*, 42(9), 1434-1443.

Woodget, A.S., Austrums, R., Maddock, I.P. and Habit, E., 2017. Drones and digital photogrammetry: From classifications to continuums for monitoring river habitat and hydromorphology. *Wiley Interdisciplinary Reviews: Water*, *4*(4).

Yoon, Y., Durand, M., Merry, C.J., Clark, E.A., Andreadis, K.M. and Alsdorf, D.E., 2012. Estimating river bathymetry from data assimilation of synthetic SWOT measurements. *Journal of Hydrology*, *464*, pp.363-375.

Table 1. Site survey characteristics for the three study sites

	River Sprint	Afon Elwy	River Ehen
Model extent (km^2)	0.148	0.173	0.164
Survey height (m AGL)	30	30	30
Images used	650	642	643
Final Model resolution (m)	0.020	0.024	0.021
Total number of points	391,871,123	387,382,170	496,849,445
GCP accuracy (m)	0.012	0.011	0.019
Field survey time (hours)	3.5	3	2.5
Post-processing time (Hours)	8.1	9.5	12.5

Table 2. Measured water depth data characteristics for the three study sites

		River Sprint			Afon Elwy			River Ehen		
Total number of data points		188			204			327		
Mean depth (m)		0.49			0.24			0.63		
Minimum depth (m)		0.02			0.02			0.15		
Maximum depth (m)		0.96			0.71			2.57		
		Min	Mean	Max	Min	Mean	Max	Min	Mean	Max
Hydraulic habitat (data points) (m)	Pool	0.13	0.62	0.96	0.02	0.33	0.71	1.01	1.22	2.57
	Glide	0.65	0.78	0.88	0.12	0.26	0.61	0.70	0.86	0.99
	Run	0.07	0.56	0.95	0.03	0.19	0.44	0.51	0.59	0.69
	Riffle	0.02	0.24	0.58	0.02	0.18	0.58	0.16	0.34	0.49
	Chute	0.12	0.38	0.90	0.12	0.23	0.41	0.15	0.49	0.66
	Back-water	0.69	0.83	0.96	0.03	0.35	0.63	n/a	n/a	n/a

Table 3. Linear regression multipliers on sUAV depth error estimates for the study sites on the River Sprint, Afon Elwy and River Ehen.

	Pool	**Backwater**	**Glide**	**Run**	**Riffle**	**Chute**
Sprint	0.73	1.08	0.9	0.87	0.98	0.76
Elwy	0.8	0.97	0.87	0.68	0.95	0.66
Ehen	0.86	not present	0.87	0.86	1.17	0.57

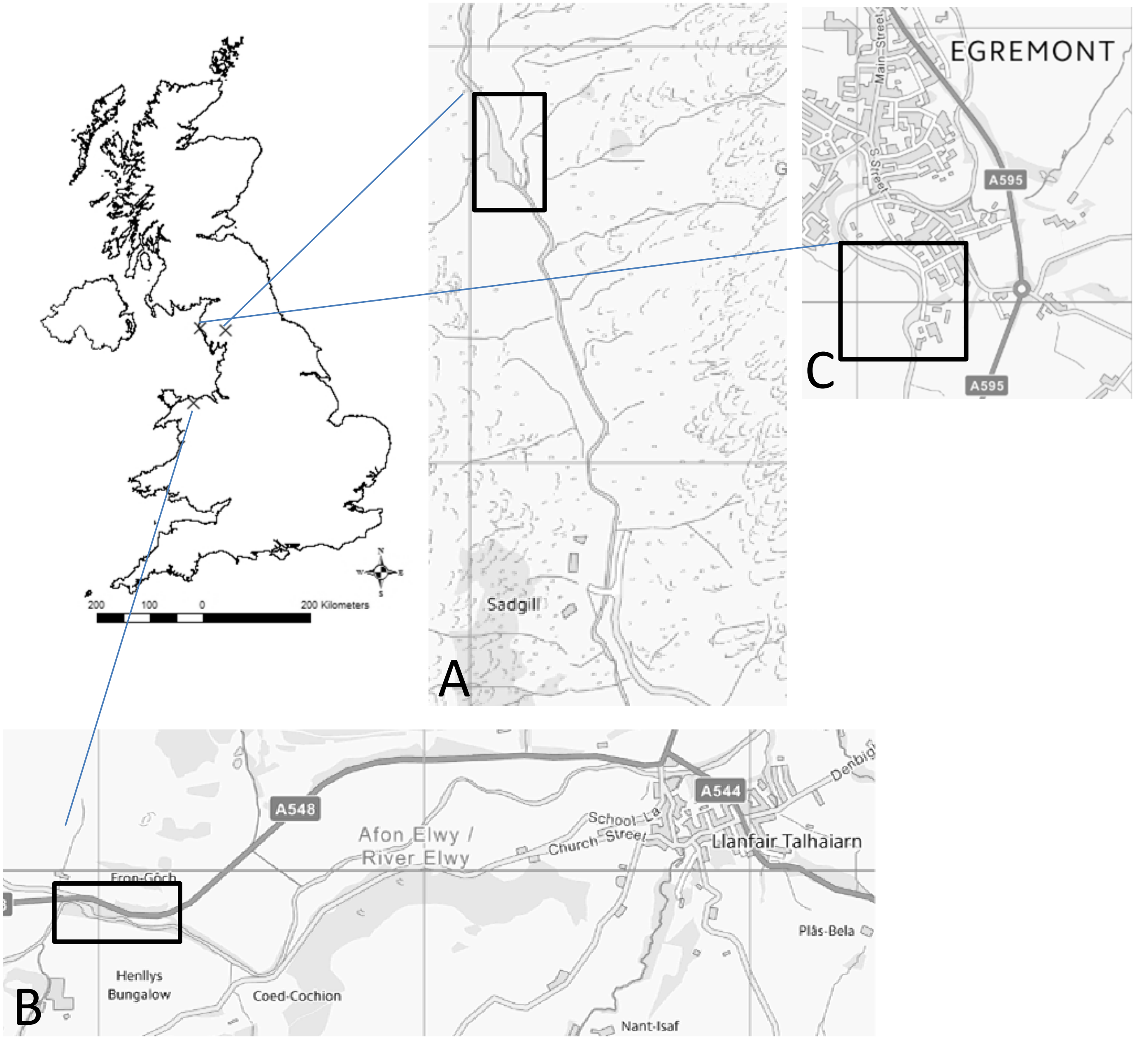

Figure 1. Location for the three sites used in this study to reflect a diversity of fluvial environments, A) River Sprint, Cumbria, England. B) Afon Elwy, North Wales, C) River Ehen, Cumbria, England.

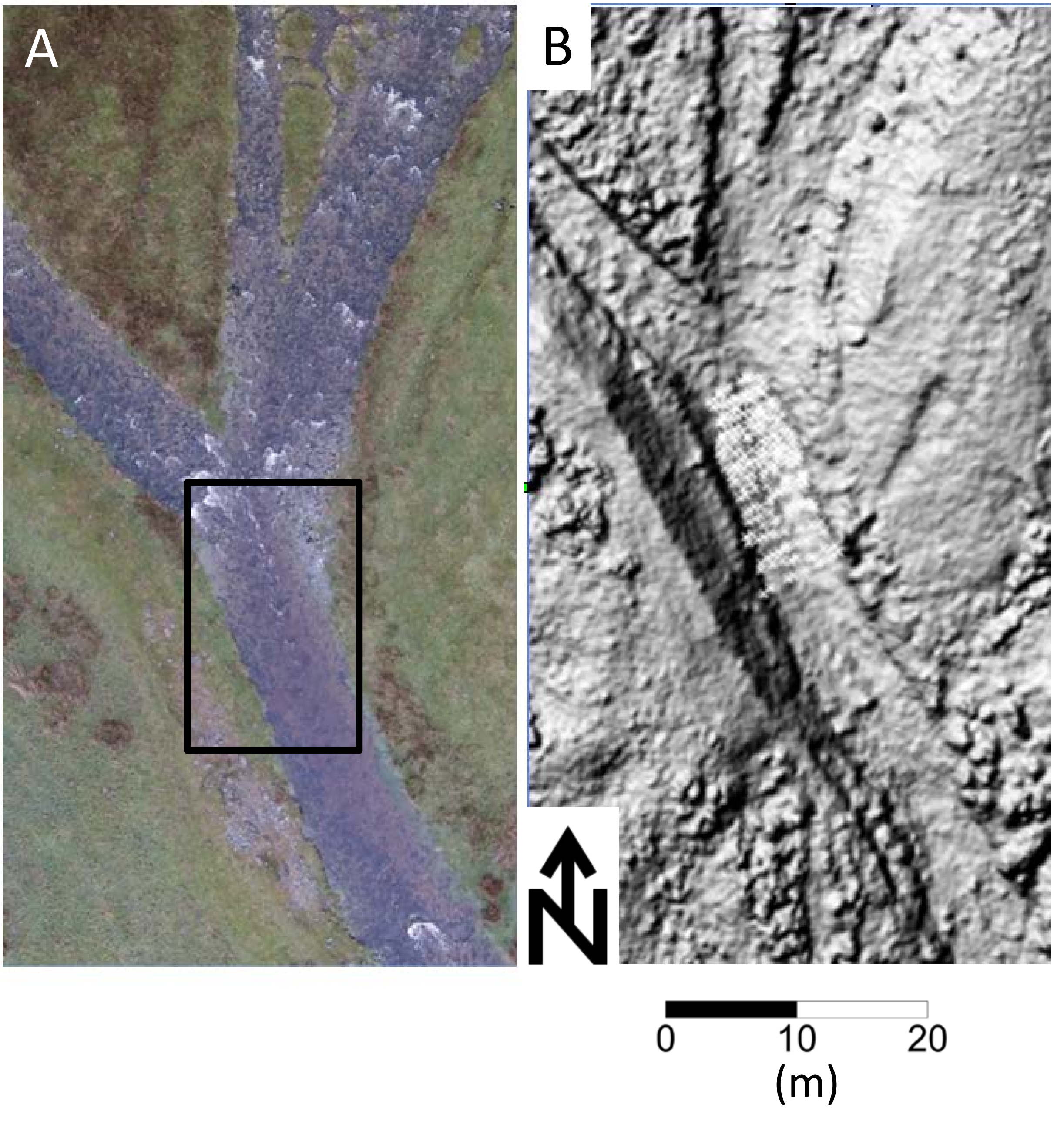

Figure 2. River Sprint sUAV derived orthophoto (A) and Digital Terrain Model (B) including boundary of pool area used for bathymetry data analysis.

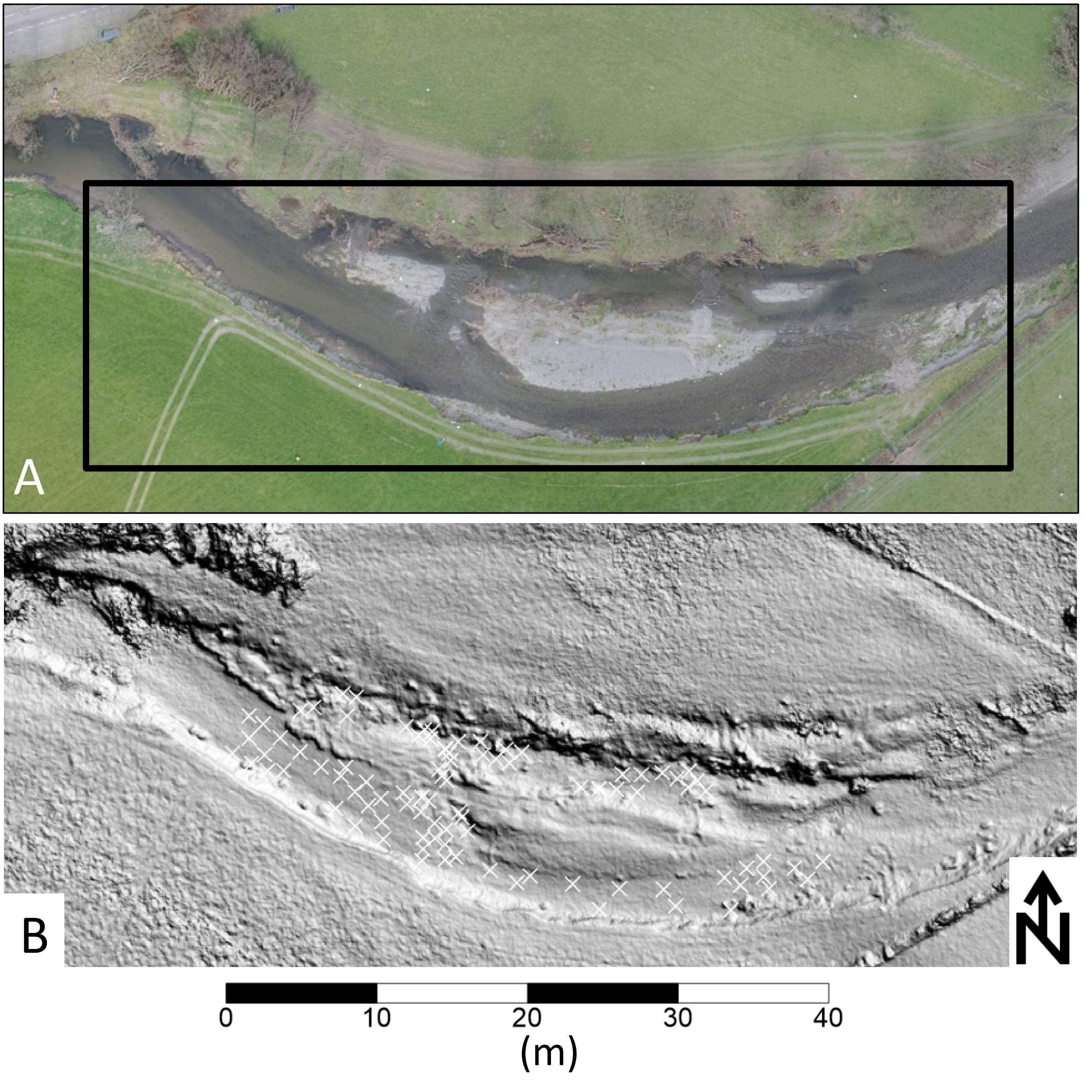

Figure 3. Afon Elwy sUAV derived orthophoto (A) and Digital Terrain Model (B). Inset image delimits the area used for biotope-based bathymetry data analysis.

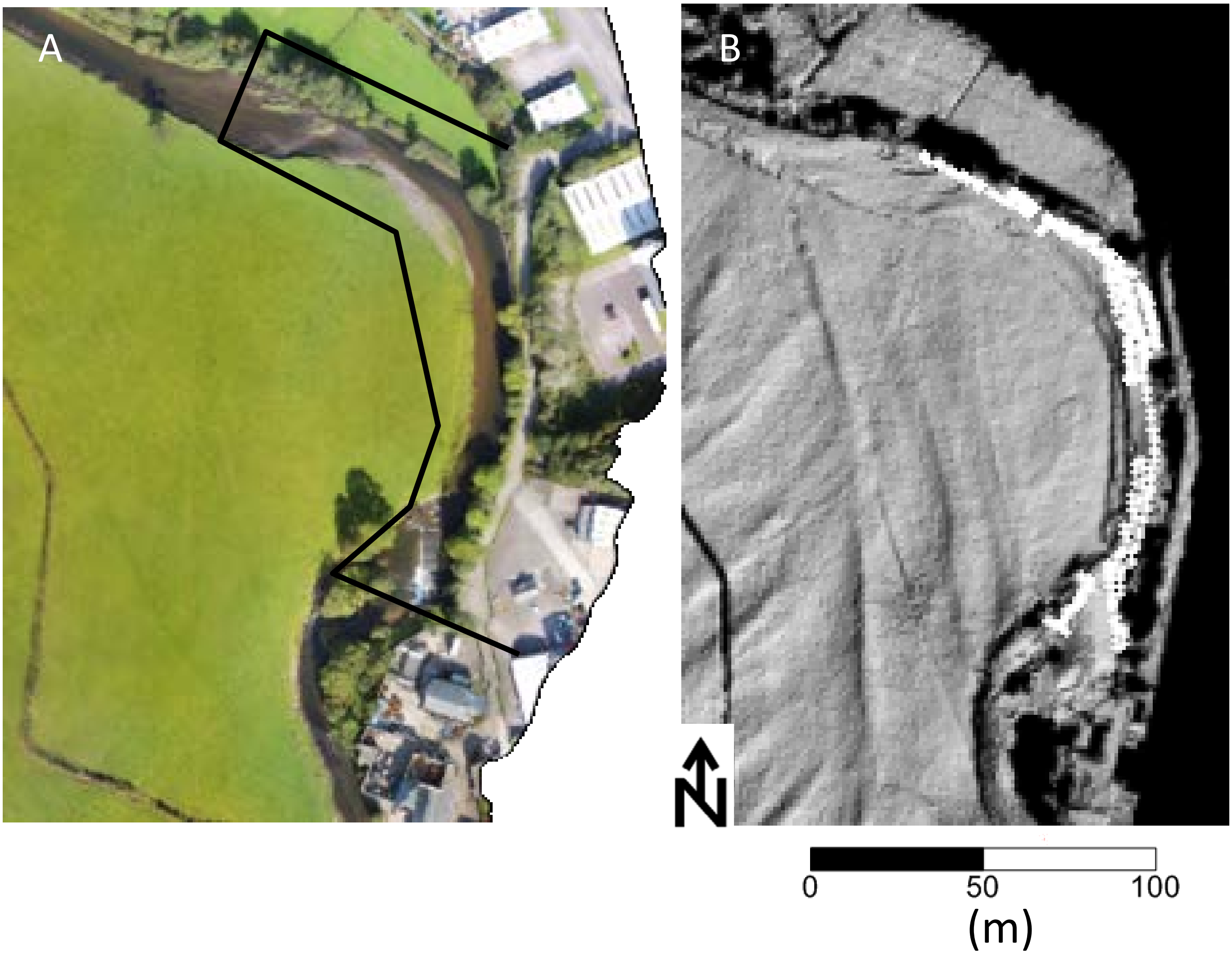

Figure 4. River Ehen sUAV derived orthophoto (A) and Digital Terrain Model (B) showing the area used for bathymetry data analysis.

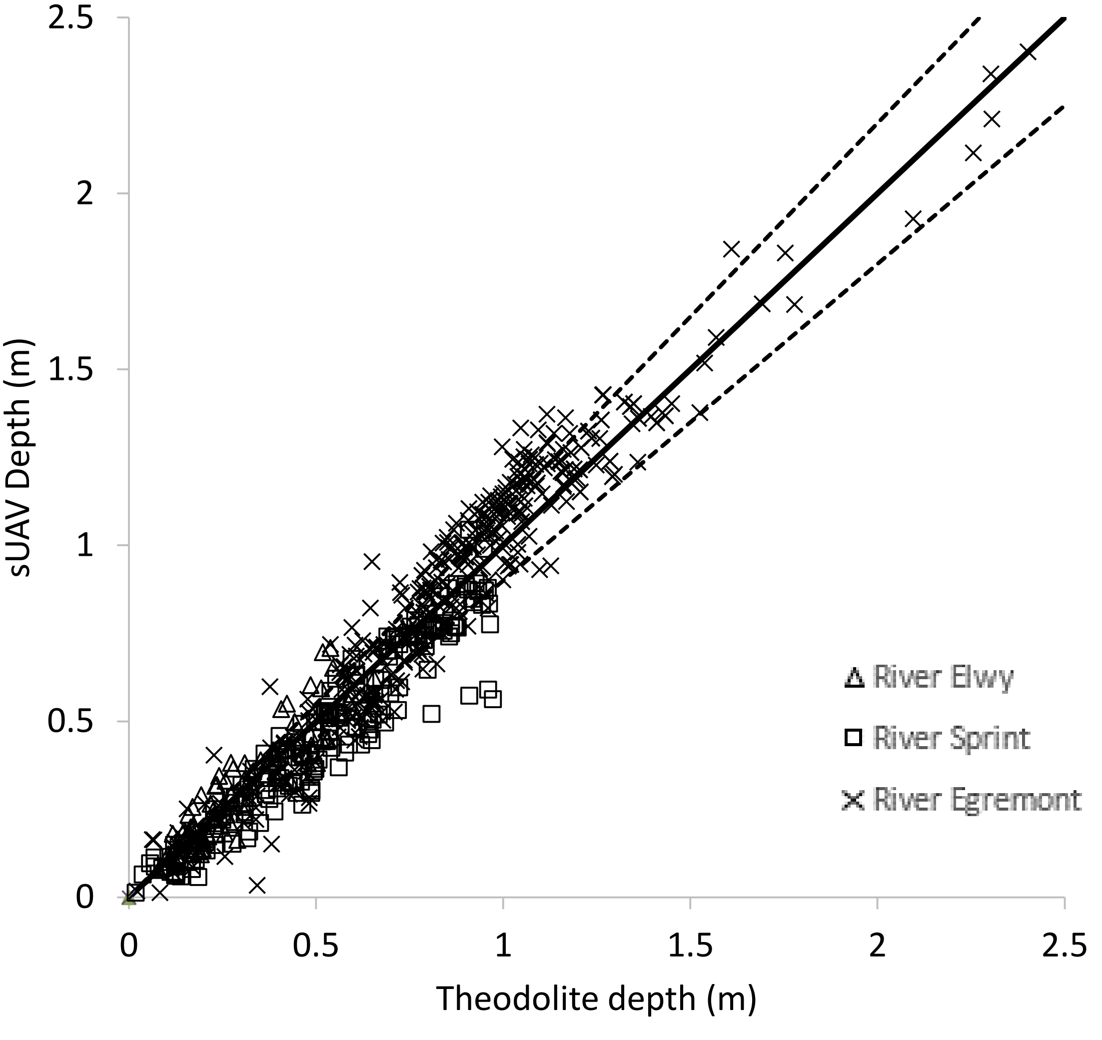

Figure 5. Comparative theodolite and sUAV depth data for the three study rivers. The solid line represents equality and dashed lines ±10% difference.

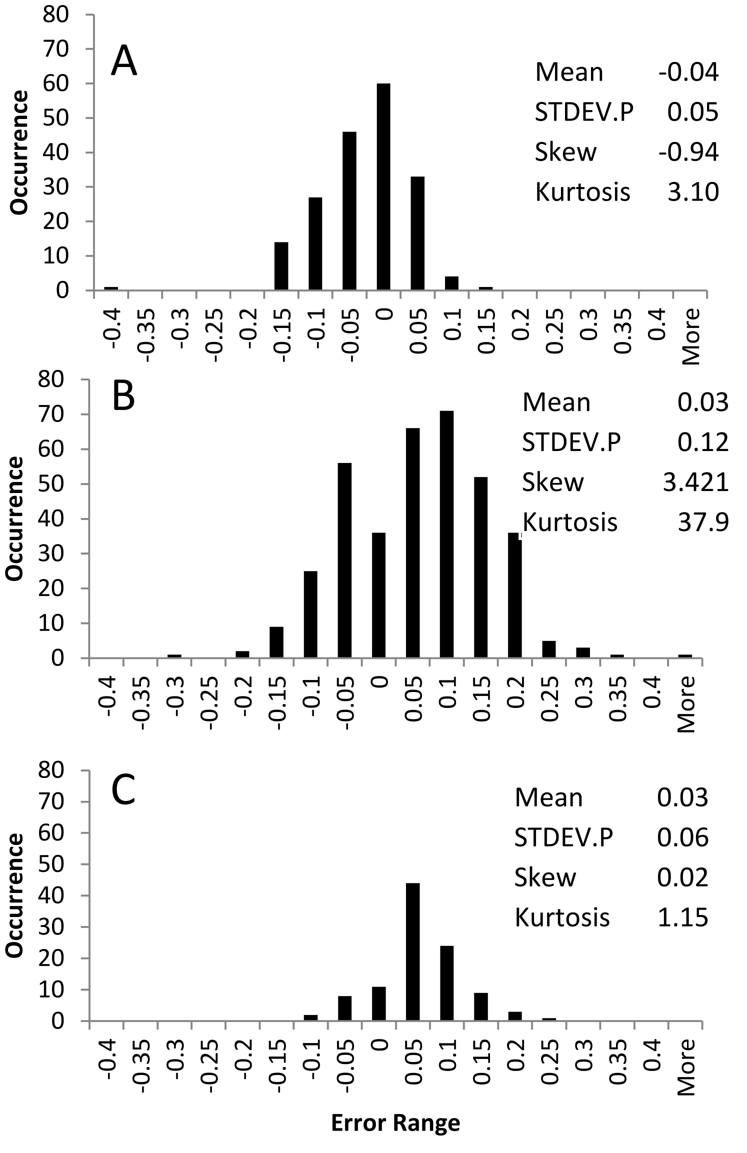

Figure 6. Theodolite and sUAV estimate depth discrepancy for Rivers Sprint A) Ehen B) and Elwy C).

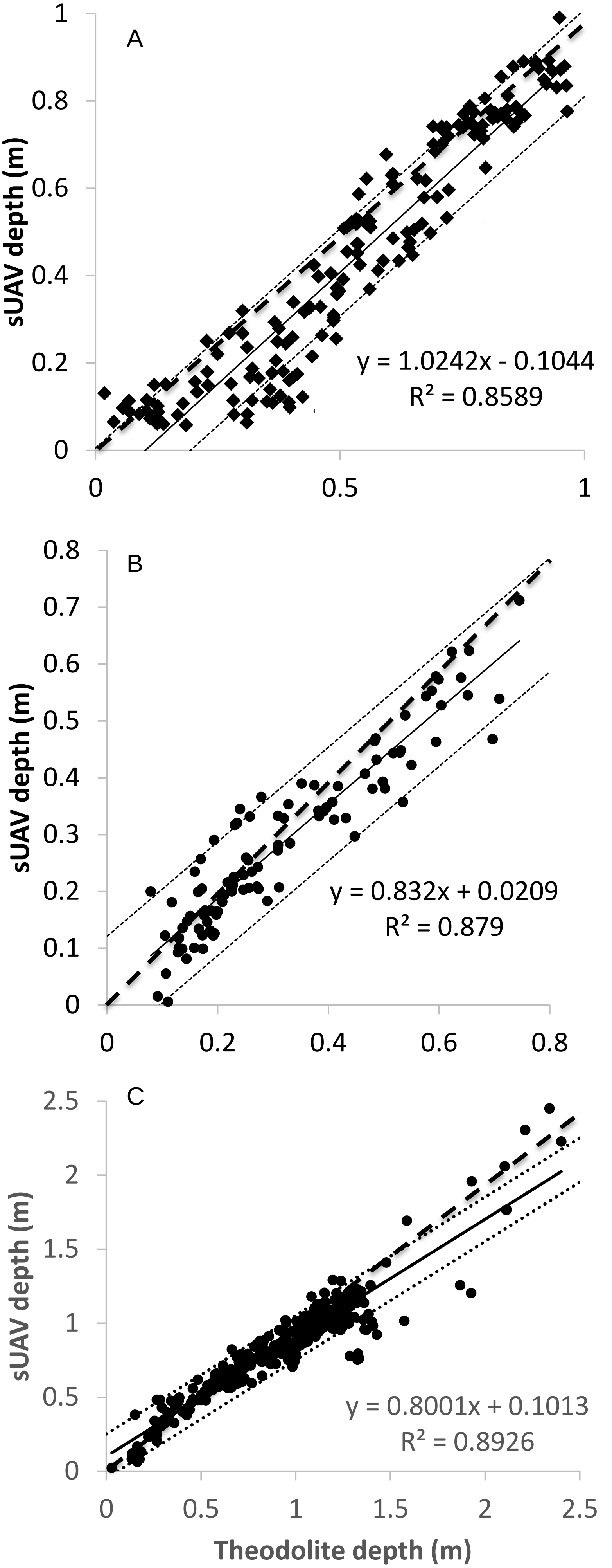

Figure 7. sUAV model estimate depth discrepancy relationship with measured depth for the a) River Sprint, b) Afon Elwy and c) River Ehen. Solid line represents equality, dashed lines show deviation equivalent to the D_{84} grain size.

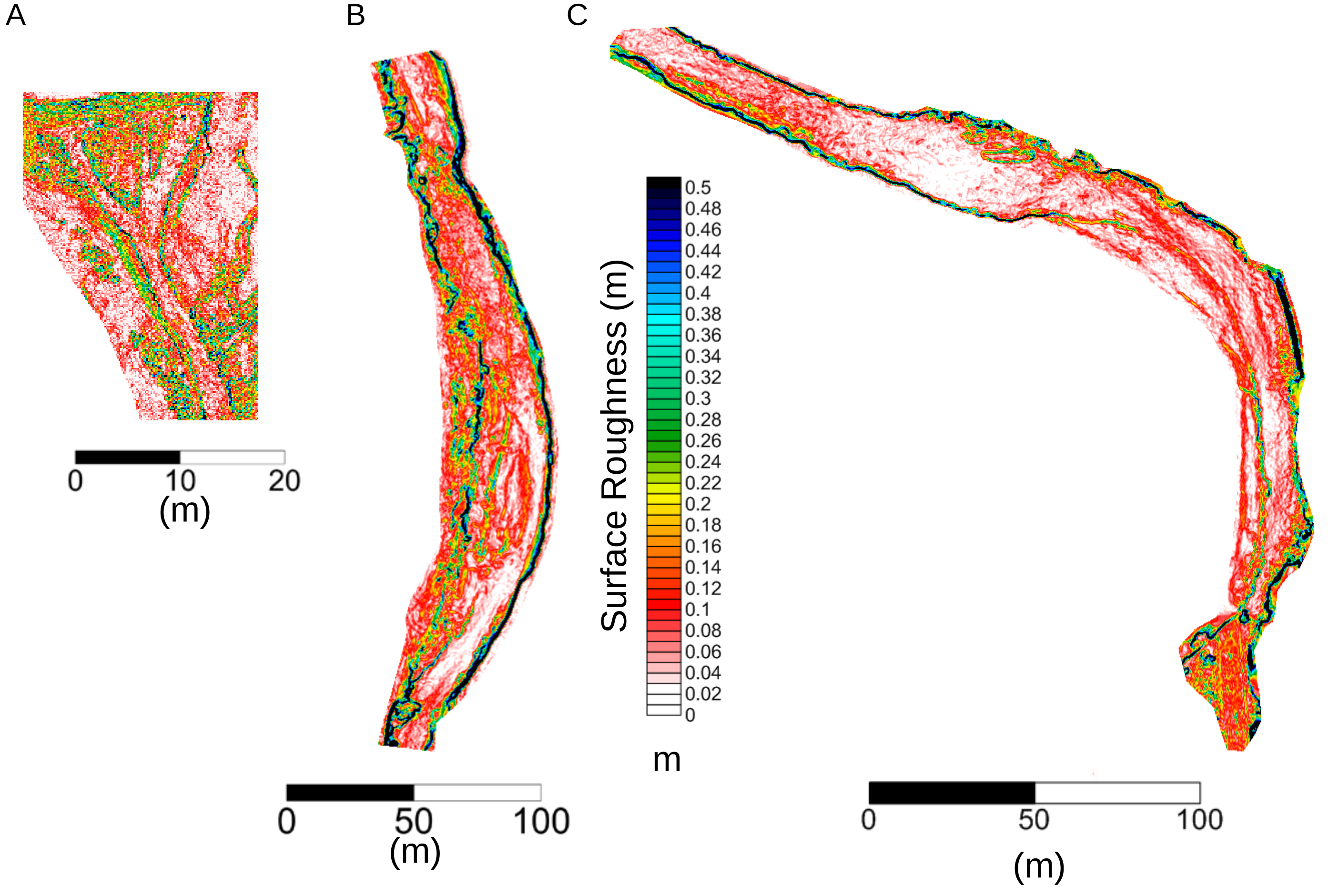

Figure 8. Bed roughness characteristics across a) River Sprint, b) Afon Elwy and c) River Ehen.

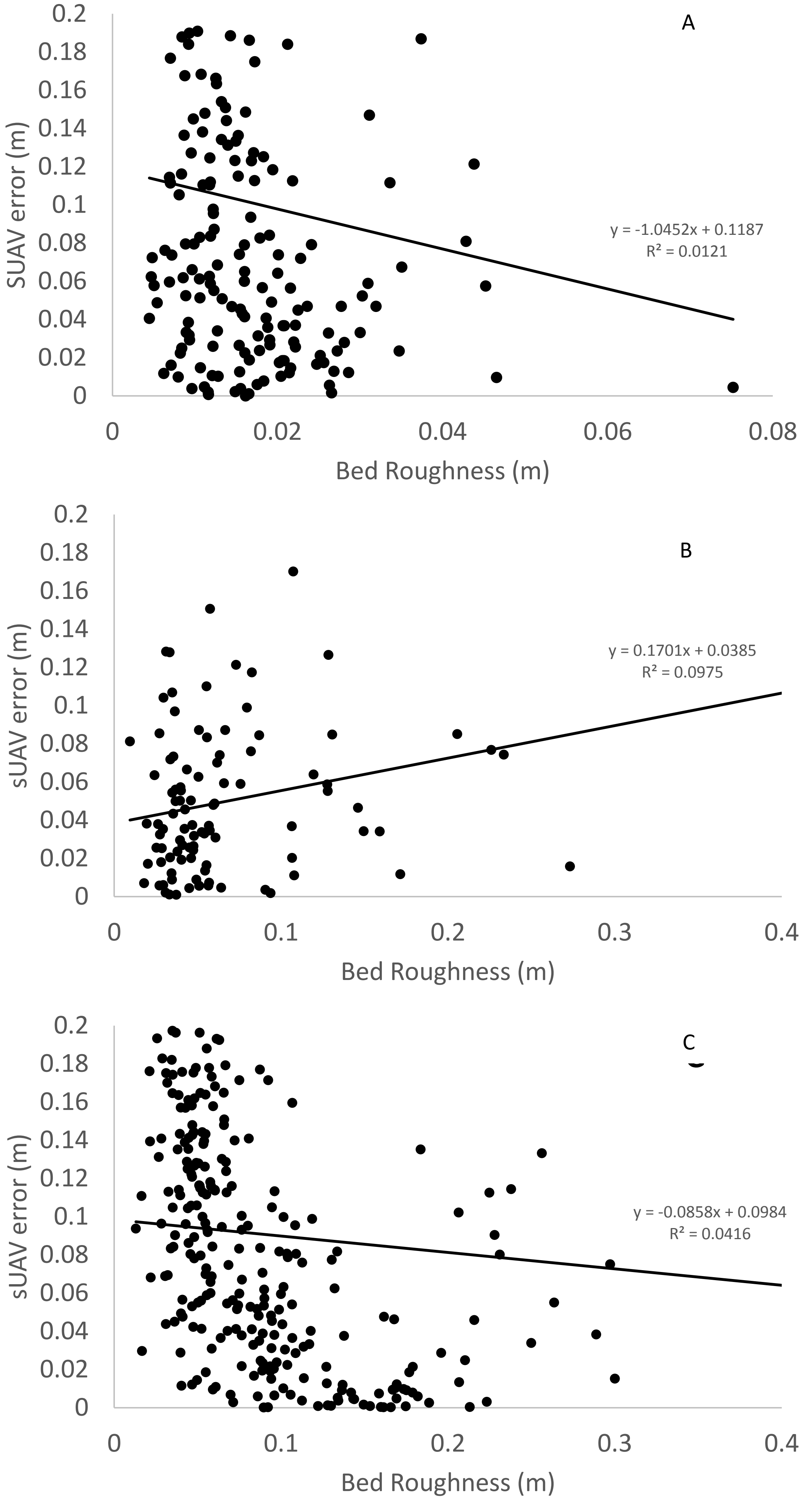

Figure 9. Local bed roughness associated with measured sUAV error across a) River Sprint, b) Afon Elwy and c) River Ehen.

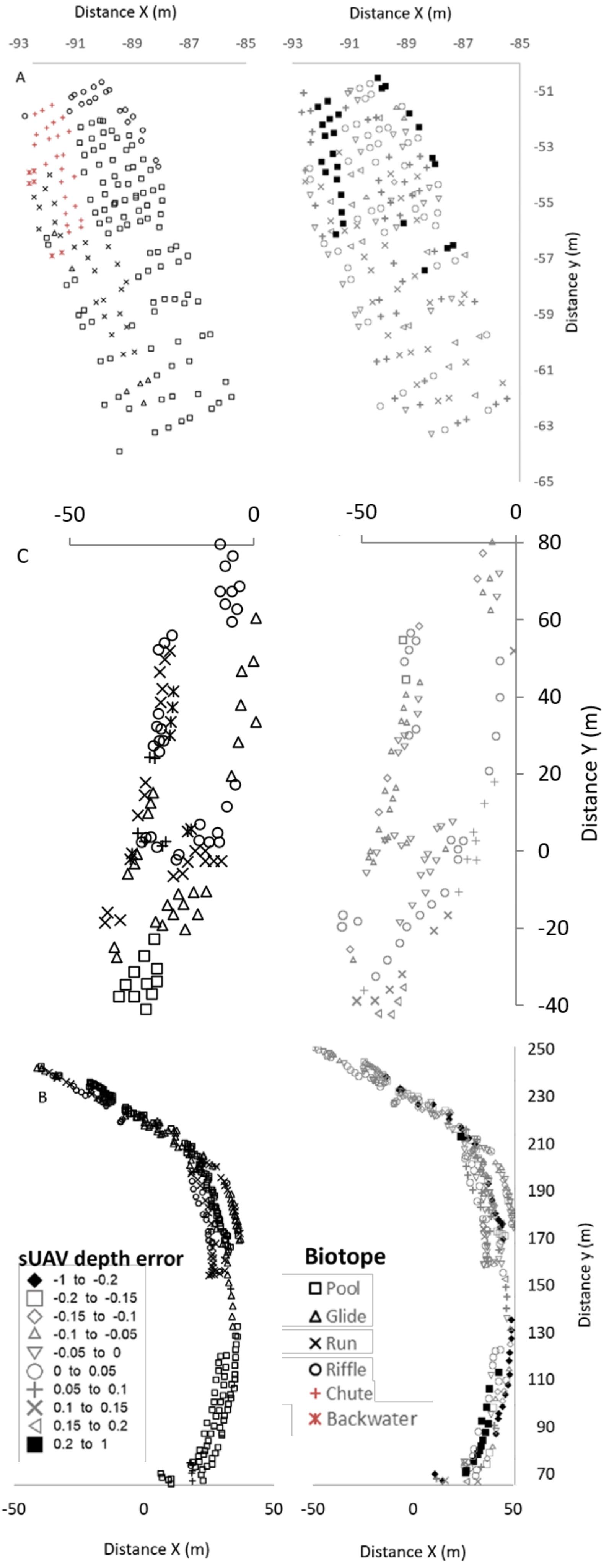

Figure 10. Water surface roughness and sUAV depth error on a) River Sprint, b) Afon Elwy and c) River Ehen.

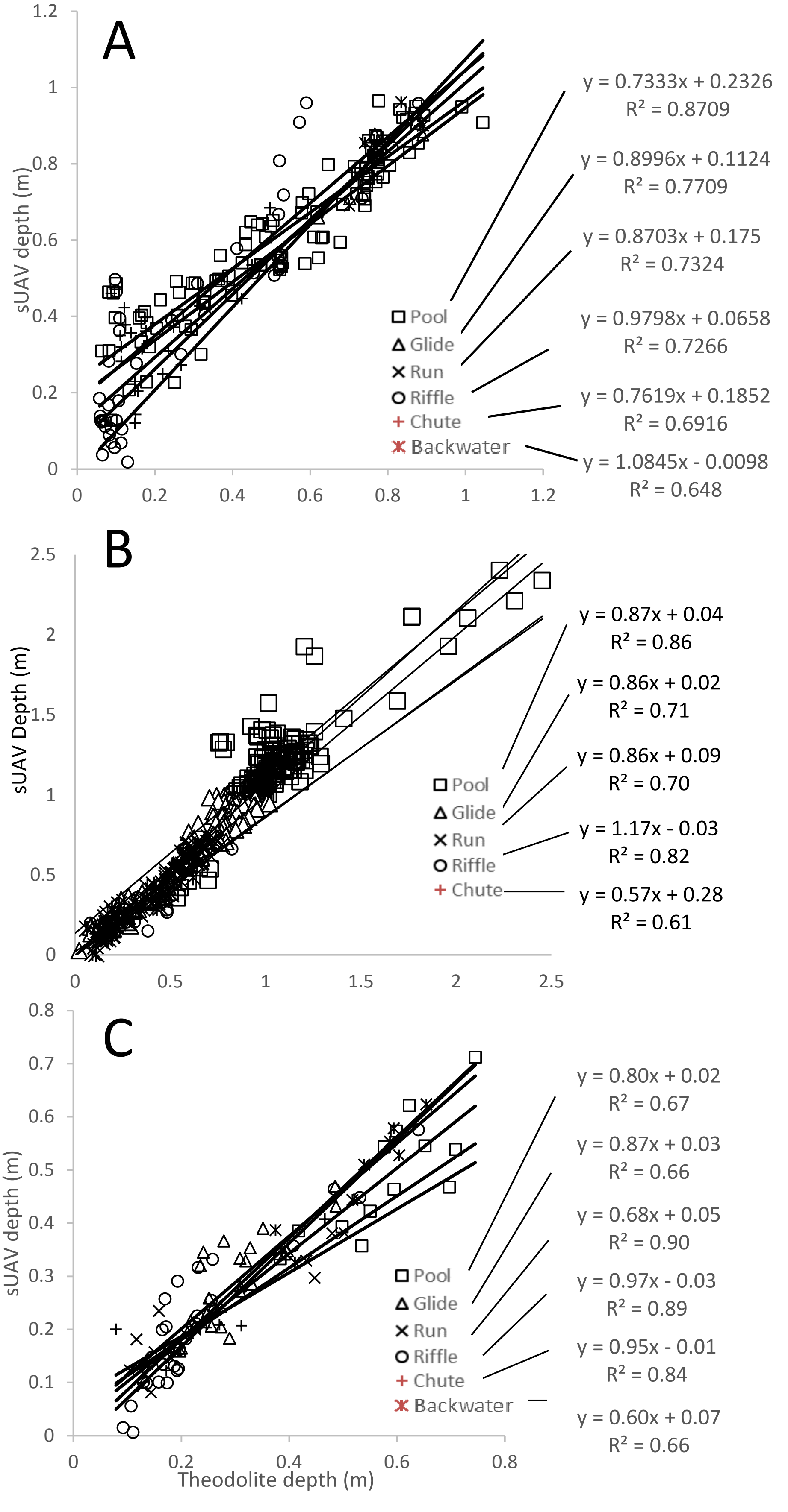

Figure 11. sUAV and theodolite depth measurements split by hydraulic biotope for a) River Sprint, b) Afon Elwy and c) River Ehen.